Journal of Chromatography A, 1218 (2011) 3360–3366

Contents lists available at ScienceDirect

Journal of Chromatography A

journal homepage: www.elsevier.com/locate/chroma

Performance evaluation of long monolithic silica capillary columns in gradient liquid chromatography using peptide mixtures

Hamed Eghbali[a,*], Koen Sandra[b], Frederik Detobel[a], Frederic Lynen[c], Kazuki Nakanishi[d], Pat Sandra[b,c], Gert Desmet[a]

[a] Vrije Universiteit Brussel, Department of Chemical Engineering, Pleinlaan 2, B-1050 Brussels, Belgium
[b] Research Institute for Chromatography, Kennedypark 20, B-8500 Kortrijk, Belgium
[c] Ghent University, Lab of Separation Sciences, Department of Organic Chemistry, Krijgslaan 281 (S4), B-9000 Ghent, Belgium
[d] Kyoto University Kitashirakawa, Department of Chemistry, Graduate School of Science, Sakyo-ku, Kyoto 606-8502, Japan

ARTICLE INFO

Article history:
Available online 15 October 2010

Keywords:
Silica monolith
Long capillary column
Gradient liquid chromatography
Peak capacity
Bed homogeneity

ABSTRACT

A systematic study is reported on the performance of long monolithic capillary columns in gradient mode. Using a commercial nano-LC system, reversed-phase peptide separations obtained through UV-detection were conducted. The chromatographic performance, in terms of conditional peak capacity and peak productivity, was investigated for different gradient times (varying between 90 and 1320 min) and different column lengths (0.25, 1, 2 and 4 m) all originating from a single 4 m long column. Peak capacities reaching values up to $n = 10^3$ were measured in case of the 4 m long column demonstrating the high potential of these long monoliths for the analysis of complex biological mixtures, amongst others. In addition, it was found that the different column fragments displayed similar flow resistance as well as consistent chromatographic performance in accordance with chromatographic theory indicating that the chromatographic bed of the original 4 m long column possessed a structural homogeneity over its entire length.

1. Introduction

After their introduction in the 1990s, silica monoliths have attracted increased attention in the field of liquid chromatography as an alternative support structure to particulate columns [1–3]. Silica monoliths have a skeleton-shaped continuous morphology and are synthesized *in situ* using the classical sol–gel technology [4]. As a result, the conventional packing procedure requiring retaining frits is avoided. In addition, the bed morphology which is often characterized by the external porosity and the domain size (comprising the skeleton and through pore size) can be tuned by controlling the initial sol–gel composition. Doing so, a second generation of silica monoliths, having a smaller domain size and increased phase ratios, was produced by Tanaka et al. [5] characterized by an increased chromatographic performance. Using alkylbenzene mixtures, plate height values of less than 5 μm were reported and attributed to the reduced mass transfer distances inside the monolithic column.

The control that can be exerted on the bed morphology by adjusting the preparation conditions also offers the possibility to produce monolithic columns having an open-porous morphology delivering a low pressure drop. This specific feature allows employing longer columns in order to further increase the chromatographic performance while maintaining a reasonable mobile phase flow at the same operation pressure. Very recently, the high performance of such long columns reaching a length of 4 m was illustrated by Tanaka et al. [6]. They demonstrated the applicability of long silica monolithic columns to achieve a striking chromatographic performance in isocratic mode going up to 1000,000 plates.

Since there is a high demand for an increased separation performance in the field of proteomics [7,8], monolithic silica capillary columns have also been explored for the separation and identification of complex peptide mixtures. While early reports focused on shorter columns [9,10], more recent papers deal with the use of long monolithic columns to further enhance the chromatographic performance and increase the number of identified peptides/proteins [11,12].

To our knowledge, detailed systematic studies regarding the chromatographic performance of these long columns (up to 4 m) have not been reported yet in gradient mode. Gradient separations are of high importance since gradient elution is the most powerful operation mode for the separation of complex mixtures in liquid chromatography. In the present contribution reversed-

* Corresponding author. Tel.: +32 02 629 33 24; fax: +32 02 629 32 48.
E-mail address: heghbali@vub.ac.be (H. Eghbali).

0021-9673/$ – see front matter © 2010 Elsevier B.V. All rights reserved.
doi:10.1016/j.chroma.2010.10.045

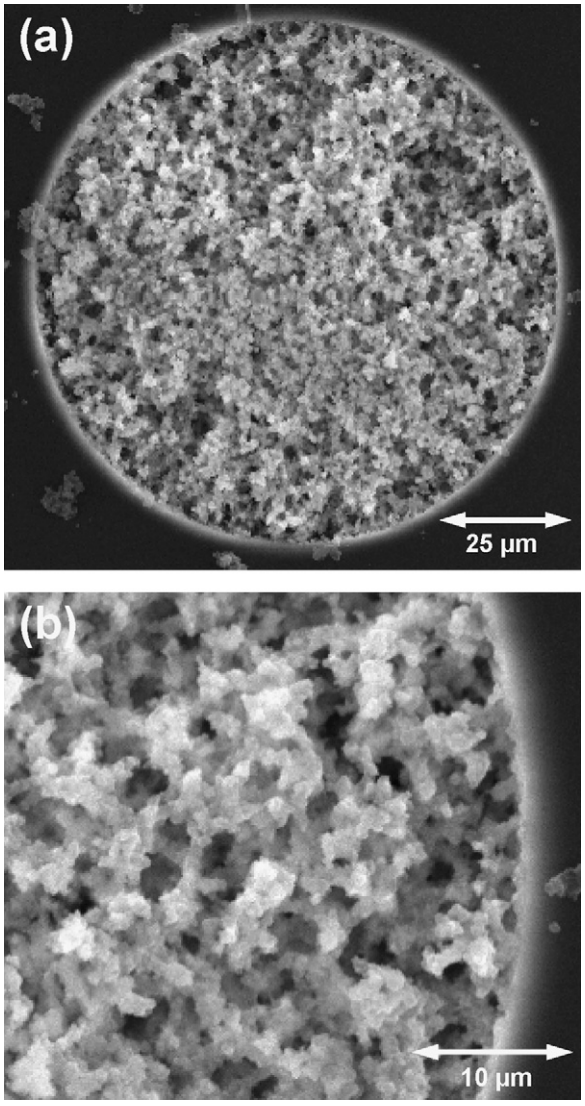

Fig. 1. SEM (scanning electron microscopy) images of the silica monolith with (a) a cross-sectional view of the monolithic capillary column (I.D.: 100 μm) and (b) a magnified view of the continuous bed morphology.

phase peptide separations obtained through UV-detection will be illustrated while applying a commercial nano-LC system at conventional pressures (below 400 bar). In almost all previous studies dealing with gradient elution, silica monoliths were exclusively evaluated or used in combination with MS [11–13]. This approach is of course much more favorable when aiming towards the identification of unknown components. UV detection is, however, more suited to study the intrinsic performance of a chromatographic bed because it is possible to exclude any biased performance contribution (the ionization source) delivered by the MS which facilitates to focus on the chromatographic performance of the column.

The chromatographic performance will be described and compared for different column lengths (ranging from 0.25 m and going up to 4 m) and gradient times. The performance was determined by measuring the conditional peak capacity based on the analysis of two different peptide mixtures (a BSA tryptic digest and a synthetic peptide mixture to allow a reliable determination of the average peak width and) under identical conditions as was previously reported by Sandra et al. [14].

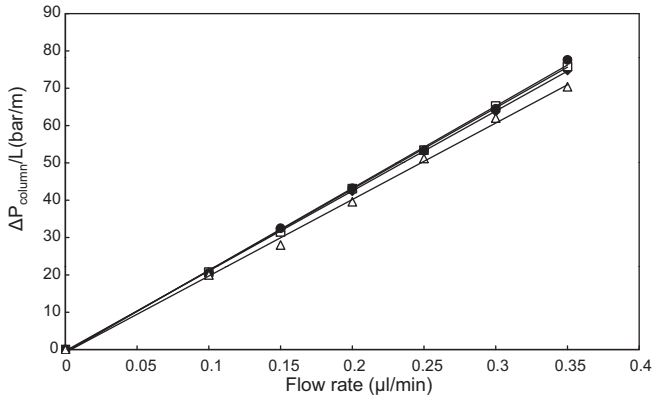

Fig. 2. Ratio between the pressure drop and column length ($\Delta P_{column}/L$) as a function of the flow rate for monolithic columns having a different column length (L): L = 0.25 m (empty triangles); L = 1 m (black dots); L = 2 m (empty squares); L = 4 m (black diamonds). The full line curves are linear regressions ($R^2 > 0.99$) of the experimental data. The pressure drops were corrected for the extra-column pressure.

The different column lengths that were investigated were obtained by cutting down the monolithic capillary column (L = 4 m) gradually into smaller lengths.

Finally, the performance of these columns will be demonstrated by a real-world proteomics sample.

2. Experimental

2.1. Materials and reagents

HPLC grade water and HPLC-S gradient acetonitrile were obtained from Biosolve (Valkenswaard, The Netherlands). Spectrophotometric trifluoroacetic acid (TFA), tris(2-carboxyethyl)phosphine (TCEP), iodoacetamide (IAA), uracil and bovine serum albumin (BSA) were purchased from Sigma–Aldrich (Bornem, Belgium). Porcine sequencing grade modified trypsin was obtained from Promega (Madison, WI, USA) and Proteomix from LaserBio Labs (Sophia-Antipolis Cedex, France).

2.2. Sample preparation

To 400 μg of BSA (~6.7 nmol), present in 100 μL 100 mM NH_4HCO_3, TCEP was added in a 50 molar excess (5 μL of a 4.75 mg/250 μL solution) and the reaction mixture was incubated during 15 min at 37 °C. TCEP is acidic and was dissolved in 500 mM NH_4HCO_3 to maintain a pH of 8. Iodoacetamide was subsequently added in a 100 molar excess (5 μL of a 6.2 mg/250 μL solution) and the mixture was incubated at 37 °C in the dark for 1 h. Iodoacetamide was dissolved in 100 mM NH_4HCO_3. The reaction mixture (in a volume of 110 μL) was subsequently desalted by means of membrane filtration (Amicon Ultra-0.5 mL, 10 kDa centrifugal filters (Millipore, Billerica, MA)). The recovered protein was subsequently diluted in 50 mM NH_4HCO_3 and trypsin was added in a 1:50 ratio (w/w) (final volume: 250 μL). Sample was incubated overnight at 37 °C and subsequently stored at −20 °C prior to analysis. A 1/5 dilution (final concentration 0.32 μg/mL) was made in 0.1% TFA prior to injection.

The peptide mixture (Proteomix containing Bradykinin, Angiotensin II, Neurotensin, ACTH, Bovine Insulin Chain B) used for the calculation of the average peak width was prepared by adding 2 mL 0.1% TFA to the lyophilized mixture. The mixture was injected as such.

The MARS depleted, reduced and alkylated human serum tryptic digest was prepared according to the procedure described in [14].

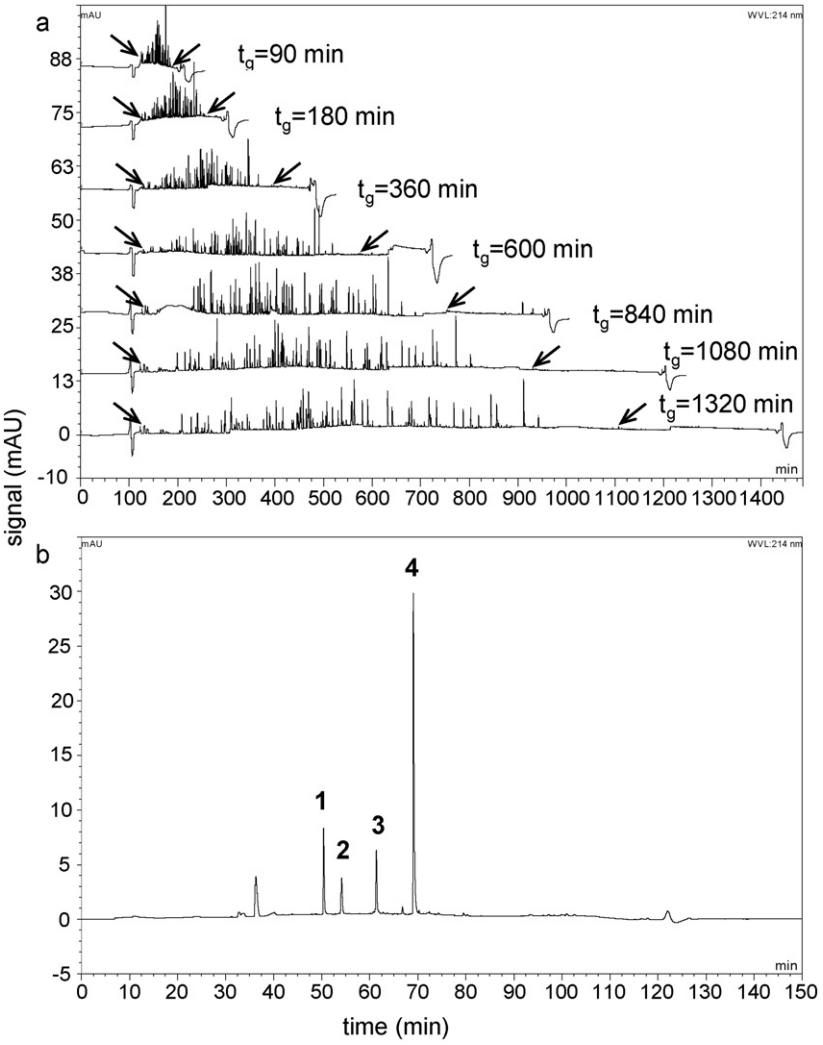

Fig. 3. Sample peak capacity determination procedure based on UV-chromatograms. (a) Separation of BSA (Bovine Serum Albumin) tryptic digest mixture for different gradient times (t_g) with a 4 m long column (FR = 0.3 μL/min). The first and last peaks chosen to calculate the separation window ($t_2 - t_1$) for implementation in Eq. (3.2) are indicated with arrows. (b) Example of a peptide test mixture separation (L = 0.25 m; FR = 0.3 μL/min; t_g = 90 min) for the measurement of the peak widths (4σ) needed to calculate the peak capacity using Eq. (3.2). The average peak width was calculated from the width of the four peaks tagged with numbers (1–4).

2.3. Instrumentation and experimental conditions

Experiments were conducted using an UltiMate 3000 Proteomics MDLC system (Dionex,Germany) with a 1:300 flow splitter and a variable-wavelength (λ = 214 nm) detector equipped with a 3-nL flow cell. The 4 m (I.D.: 100 μm) long monolithic capillary column (delivering a performance of N = 370,000 in isocratic mode with hexylbenzene (k = 0.2) as marker), fabricated at Kyoto Monotech (Kyoto, Japan), was kindly donated by GL Sciences Inc. as research sample. The different column lengths investigated, were obtained by cutting down the original monolithic capillary column (L = 4 m) gradually into smaller lengths (L = 2 m, 1 m, 0.25 m). During this process the column was each time cut at the injection side while leaving the connection (that was established by means of a zero-dead volume union (Upchurch Scientific®) to minimize any additional band broadening) between the end of the column and detector intact. Columns were operated at 300 nL/min and thermostated at 25 °C. Solvents A and B consisted of water (0.1% TFA) and 20/80-water/ACN (0.08% TFA), respectively. The extra-column pressure was measured to be 15 bar at a FR = 300 nL/min using solvent A. This was realized by connecting the injection valve directly to the UV-detector by means of a 15 cm long capillary having a large ID (150 μm), hence displaying a negligible pressure drop at the present flow rate. Theoretical calculations (not shown) also confirmed that the pressure drop over the capillary was much less than 1% of the overall measured pressure drop. Linear gradients were conducted for different gradient times (t_g = 90; 180; 360; 600; 840; 1080; 1320 min) from 0% B to 70% B followed by column regeneration and equilibration. Samples were injected in full loop mode (1 μL). Chromeleon software (Dionex) was used for data acquisition and analysis.

3. Results and discussion

3.1. Morphology and pressure drop

Fig. 1 shows a cross-sectional view of the monolithic column that was investigated in the current study. The continuous skeleton-shaped morphology which is typical for silica monoliths can be clearly observed. Based on several SEM-images (Fig. 1), the skeleton size and through-pore size could be roughly estimated to be 1–2 μm and 3–4 μm, respectively, resulting in a domain size around d_{dom} = 5 μm. Comparing the estimated through-pore size with the through-pore size of a conventional bed packed with 5 μm particles ($d_{por} \cong (d_{part}/3) \cong 1.7$ μm), it can be concluded that the through-pore of the presently used monolith is relatively large (two

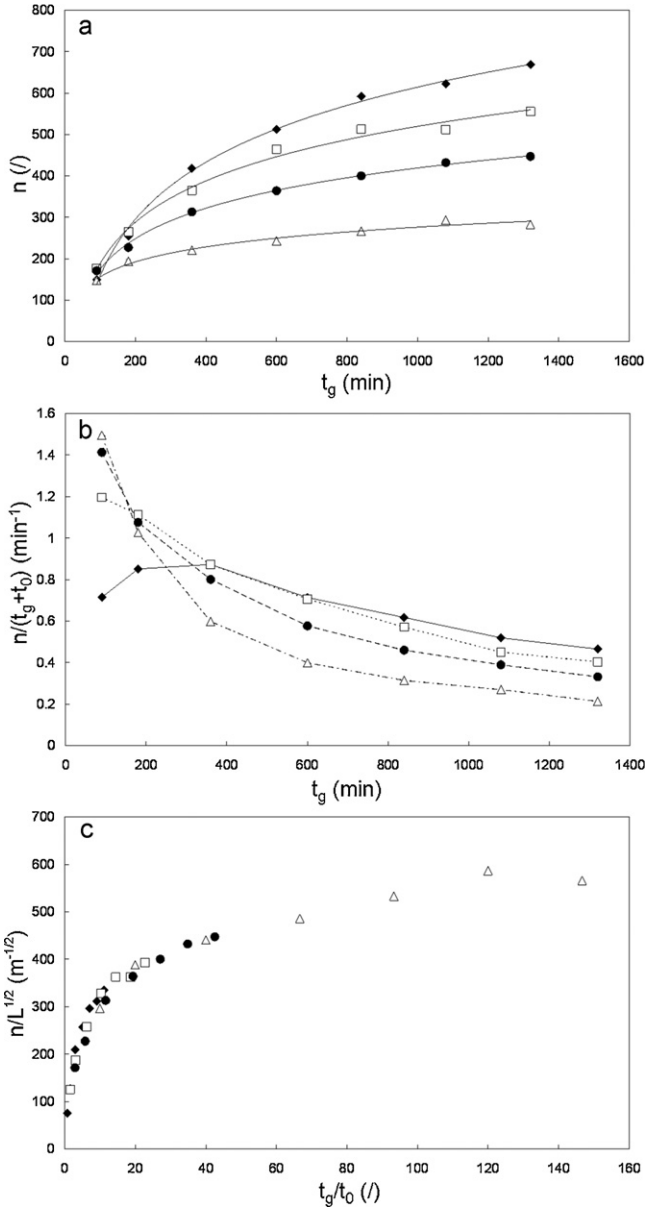

Fig. 4. (a) Peak capacity (n) as a function of the gradient time (t_g) for monolithic columns (FR = 0.3 μL/min) having a different column length (L): L = 0.25 m (empty triangles); L = 1 m (black dots); L = 2 m (empty squares); L = 4 m (black diamonds). The full line curves are added to guide the eye. (b) Plot of the peak productivity ($n/(t_g + t_0)$) as a function of the gradient time (t_g) for the different column lengths. The full line curves are added to guide the eye. (c) Same experimental data as in (a) where $n/L^{1/2}$ *vs.* t_g/t_0 is plotted. The column dead time (t_0) of the different columns was determined using uracil as tracer component. All data points result from triplicate measurements.

times larger). This observation underlines the open-porous character of these monoliths making them suitable for the construction of longer columns.

The permeability of the initial 4 m long monolith was determined to be $K_{v0} = 11 \times 10^{-14}$ m^2 which is in the same range as the permeability of the long monolithic columns described by Tanaka et al. [6]. The relationship between the pressure drop and the flow rate can be depicted as:

$$\frac{\Delta P_{\text{column}}}{L} = cst\, F \tag{3.1}$$

where ΔP_{column} is the pressure drop over the column; L represents the column length and F the flow rate. The value of the proportional constant (cst) is a measure for the flow resistance of the chromatographic bed.

Fig. 2 shows a plot where $\Delta P_{\text{column}}/L$ is plotted *versus* F for the different column lengths (L = 0.25 m; 1 m; 2 m; 4 m) in isocratic mode (100% solvent A). For all four different column lengths a clear linear trend ($R^2 > 0.99$) can be observed which is consistent with Eq. (3.1). It should be mentioned that the pressure drops have been corrected for the extra-column pressure. In case of the smallest column (L = 0.25 m) an overall pressure drop of 30 bar was assessed at a flow rate of 0.3 μL/min. Half of this total pressure drop (15 bar) could be attributed to the extra-column pressure. This implies that the extra-column pressure contributes significantly to the total pressure drop and should not be neglected, especially for the shorter columns where this contribution is more pronounced.

Another striking assessment in Fig. 2 is the good overlap of the four curves. Interpreting this observation using Eq. (3.1), it can be derived that the flow resistance (which is proportional to the slope of the curve) for all four cases are identical within a relative standard deviation of three percent. This leads to the conclusion that the original 4 m long monolithic column exhibited structural homogeneity over its entire length regarding flow resistance.

3.2. Chromatographic performance

The chromatographic performance of the different monolith columns were quantified by measuring the sample peak capacity n [15]:

$$n = \frac{t_2 - t_1}{W_{\text{av}}} \tag{3.2}$$

where t_1 and t_2 are, respectively, the retention times of the first and the last eluting components in the sample. W_{av} represents the average peak width (4σ) of selected peaks eluted within this time window.

Later on, the term *conditional* peak capacity was used for the same concept to emphasize that its value strongly depends on all experimental conditions including gradient program, column parameters as well as the employed sample(s) [16].

The currently employed method to determine the conditional peak capacity is similar to the procedure reported by Sandra et al. [14]. First, a BSA tryptic digest as injection sample was analyzed (Fig. 3a). The retention window which is the nominator in Eq. (3.2) could be easily derived from the obtained chromatograms. However, since we are dealing with a highly complex mixture, the accurate determination of the average peak width is difficult and less reliable because partial or complete peak overlap can occur and influence the measured average peak width. When exploring different gradient conditions, selectivity changes have also been reported [17]. This makes identification of the selected peaks from one chromatogram to another much more difficult. Therefore, a commercially available standard peptide mixture was separated under identical conditions as the BSA digest mixture (while eluting within the separation window of the BSA digest) and used to determine the average peak width (W_{av}) for implementation in Eq. (3.2). Fig. 3b shows a separation of the peptide mixture at the lowest separation condition (L = 0.25 m; t_g = 90 min) that occurred in the present study. The use of such a standard peptide mixture for the calculation of the peak capacity has several advantages compared to complex mixtures. On the one hand, the sample components can be easily resolved and hence allow for a baseline separation of the different peaks. That way the peak widths can be easily measured with minimal bias, even when dealing with relatively low performance separation conditions (Fig. 3b). On the other hand, a good peak shape in combination with an optimal signal-to-noise ratio can be achieved which again facilitates a prompt derivation of the peak width from the recorded chromatograms.

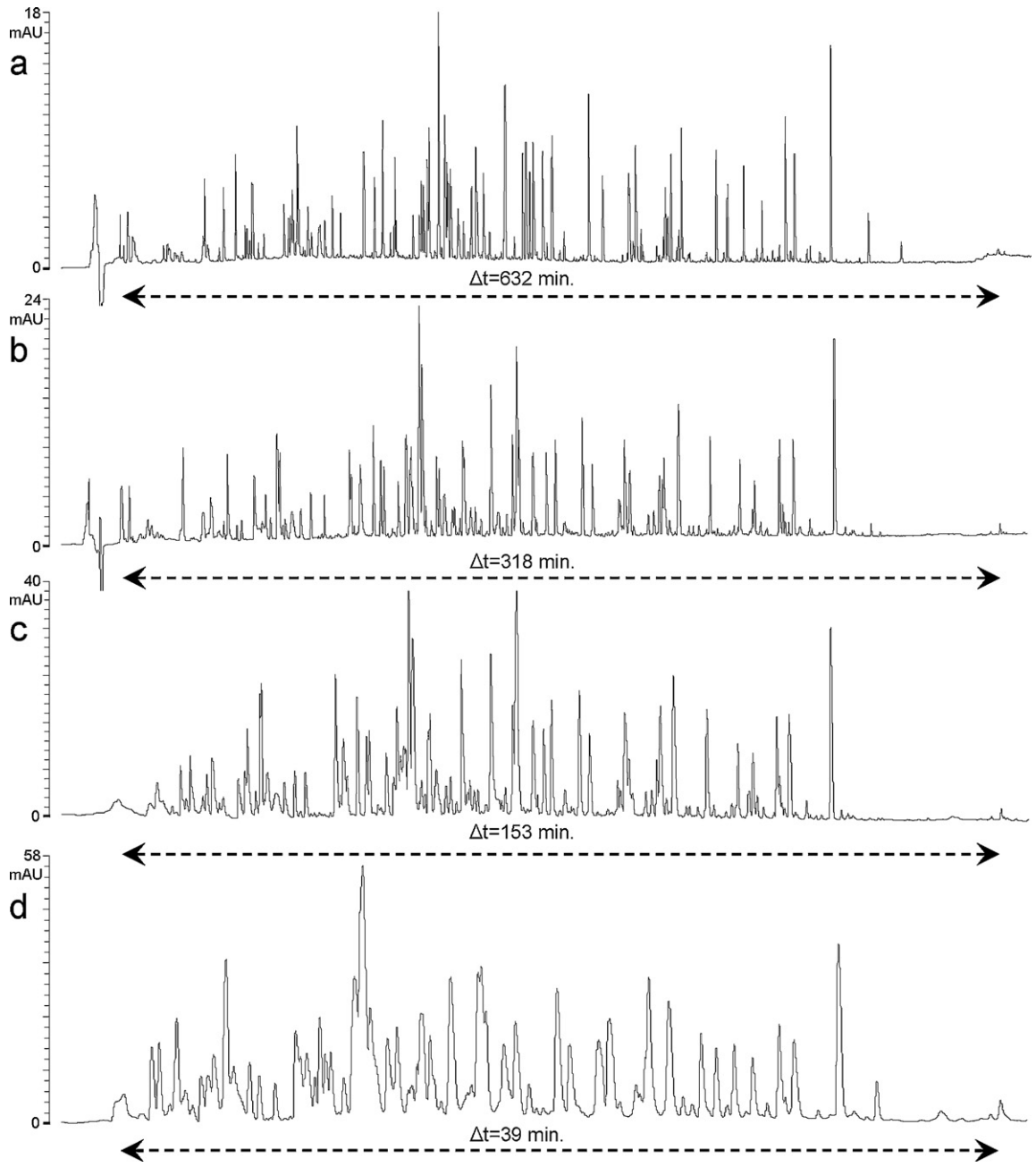

Fig. 5. Separation of BSA tryptic digest mixture with four different column lengths (FR = 0.3 μL/min). To obtain similar retention factors for the different components, the gradient time was adjusted proportionally to the column length (corresponding to a constant t_g/t_0-ratio for all four columns). With (a) $L = 4$ m ($t_g = 840$ min); (b) $L = 2$ m ($t_g = 420$ min); (c) $L = 1$ m ($t_g = 210$ min); (d) $L = 0.25$ m ($t_g = 52.5$ min).

Fig. 4a shows the progress of the peak capacity *versus* the gradient time for the four column lengths. At short gradient times the peak capacity increases rapidly, while at higher gradient times this increase becomes less significant. This qualitative trend of the peak capacity as a function of the gradient time corresponds well with the trend predicted by gradient elution theory [18].

It should be noted that the peak capacities for the different column lengths have the tendency to overlap at low gradient times ($t_g = 90$ min) implying that no gain in absolute performance can be obtained by switching to an increased column length. In contrast, it can also be clearly observed that for the considered range of long gradient times the longer columns display a superior performance with respect to the shorter one. At $t_g = 1320$ min a conditional peak capacity going up to $n = 700$ could be achieved with the longest column ($L = 4$ m) which is a factor 2.5 higher compared to the performance of the shortest column ($L = 0.25$ m). In the past, peak capacity values of $n = 1000$–1500 have been reported using long packed capillary columns ($L = 2$ m) [19] and coupled conventional sized columns [20,21]. These methodologies required either the use of ultra-high pressures or high temperatures.

Yet, we do not intend to juxtaposition our obtained conditional peak capacity values with previously published results [19–23]. We believe that a cross-comparison of reported conditional peak capacities is unsuited since the conditional peak capacity value is by definition strongly dependent on the used sample(s) and conditions as well as on the applied method to determine the peak capacity. For instance, in some cases a single peak is used to determine the peak width [11] whereas in other cases an average of several selected peaks is taken [20,22] as in the present study.

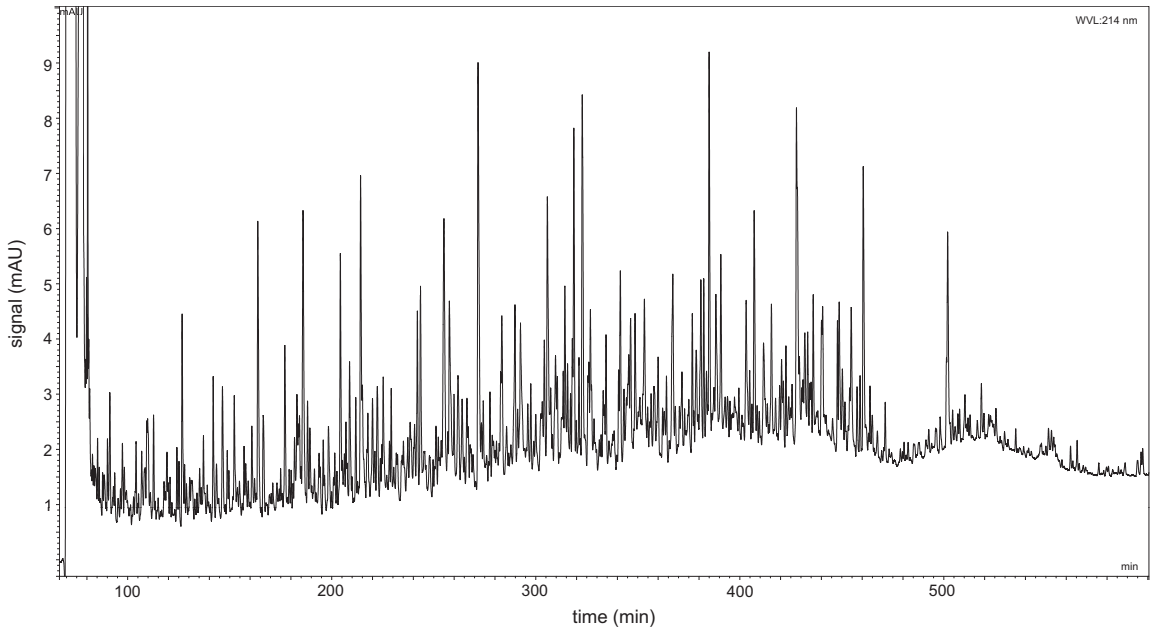

Fig. 6. Analysis of 1 μg of a healthy serum tryptic digest, depleted for the six most abundant proteins, on a 4 m long monolithic capillary column. Capillary was thermostated at 45 °C and operated at a flow rate of 0.45 μL/min. A 700 min gradient was applied between 0 and 70% B. Peak capacity value was estimated to approach 10^3.

From Fig. 4a it could be concluded that higher performance can be obtained for longer columns. Nonetheless, the price one has to pay when switching to a longer column is an increased analysis time which is a crucial aspect especially when facing routine analysis. Ultimately, the main challenge in practice remains to choose t_g for a given column length such that sufficient separation performance is obtained within a reasonable analysis time.

In order to account for the analysis time ($t_g + t_0$), the peak productivity (amount of peaks per unit of time) can be calculated as [24]:

$$\mathrm{PP} = \frac{n}{(t_g + t_0)} \tag{3.3}$$

where t_g and t_0 are the gradient time and column dead time, respectively.

Fig. 4b displays the peak productivity as a function of the gradient time. A general decreasing trend for all four column lengths is observed with increasing gradient time. This trend is caused because the conditional peak capacity has the tendency to flatten out at larger gradient times (Fig. 4a). It should be also noted that for relatively low gradient times (t_g = 90 min) a shorter column outperforms the larger columns while for large gradient times (t_g > 600 min) the situation is reversed. This observation is due to the fact that at shorter gradient times the column dead time (which is proportional to the column length) starts to dominate the analysis time ($t_g + t_0$) which is the denominator in Eq. (3.3).

In general, it can be considered that at very low gradient times the column dead time starts to be the determining factor for the value of the analysis time (denominator in Eq. (3.3)) while at higher gradient times the influence of the column dead time with respect to the analysis time is minimal. This is also the reason why at low gradient times the longest columns (having the largest t_0) exhibit the lowest PP. While the gradient time increases the effect of t_0 reduces and the longest columns delivering the highest peak capacity also display the largest PP. Since the PP is influenced by an interplay between t_g and t_0, it can be expected that the PP reaches an optimum value at a certain t_g. In Fig. 4b only for the 4 m column a clear optimum (around t_g = 300 min) can be observed in contrast to the three shorter columns. This assessment is nevertheless not surprising since the influence of the column dead time on the PP occurs at a higher t_g because the 4 m long column has the largest column dead time. Considering the same argumentation, it should be expected that the other column lengths (L = 0.25 m, 1 m, 2 m) should also reach an optimum, yet at a lower gradient times (lower than t_g = 90 min).

From Fig. 4a and b, it can be finally concluded that the value of the gradient time is a critical factor and has to be chosen sufficiently large when one aims to benefit from an increased column length. One might be disappointed upon increasing the column length while maintaining the same gradient time.

According to the theory of gradient elution it can be assumed that:

$$n \cong \sqrt{N} \cong \sqrt{L} \tag{3.4}$$

demonstrating that the conditional peak capacity is proportional to the square root of the plate number (N) which is on its turn proportional to the column length (L) [21]. Eq. (3.4) holds for reversed-phase chromatography separations when a linear solvent strength gradient is applied and when the t_g/t_0-ratio is kept constant resulting in similar retention factors for the different components in the mixture. This latter condition is fulfilled in the present study by adjusting the gradient time (t_g) proportionally to the column length (L) as the flow rate is kept constant (FR = 0.3 μL/min) [21]. As an illustration, Fig. 5 shows a BSA tryptic digest mixture separation obtained with the different column lengths. The enhanced resolving power caused by an increase in column length can be visually observed confirming the relationship between the conditional peak capacity and column length Eq. (3.4).

Going more into detail, Eq. (3.4) can also be expressed as:

$$\frac{n}{\sqrt{L}} = cst \tag{3.5}$$

This implies that the ratio of the sample peak capacity n and the square root of the length should yield a constant value for a given t_g/t_0-ratio. Fig. 4c is obtained through a simple data transformation from the experimental data shown in Fig. 4a. The perfect overlap of the data points for the four column lengths in Fig. 4c demonstrates the validity of Eq. (3.5) indicating good agreement of the experimental results with theory of gradient elution. This assessment

illustrates that the four column fragments possessed an identical structural bed homogeneity indicating that the original monolithic column having a length of 4 m was homogeneous over its entire length. Similar observations have also been reported for packed beds [21].

3.3. Real-world sample analysis

As a final illustration, the monolithic column was applied to the analysis of a real-world sample. Fig. 6 shows a separation of a human serum tryptic digest depleted for the six most abundant proteins obtained with a 4 m long monolith through UV-detection. The extreme resolving power of the column already allows observing numerous sharp peaks. The peak capacity value was estimated to approach 10^3. In future work the applicability of these columns in combination with MS-detection is going to be explored. Very recently, Ishihama et al. applied such long columns in combination with tandem mass spectrometry for the investigation of the *E. coli* proteome [12]. They were able to identify more than 22,000 tryptic peptides originating from 2602 proteins and thereby covered nearly the entire *E. coli* proteome. A question that remains to be answered is whether the high number of identified proteins is attributed to the increased peak capacity of the column or to the time available for MS/MS analysis or a combination of both phenomena. In other words, what is the relationship between chromatographic performance and the number of identified peptides/proteins.

4. Conclusion

We have presented a systematic study of the performance of long silica monolithic columns in gradient mode using peptide mixtures. Through UV-detection the performance of the columns was determined by measuring the conditional peak capacity. Different column lengths all originating from a single 4 m column were explored by determining the chromatographic performance at different gradient times.

When sacrificing analysis time, a conditional peak capacity of $n = 700$ could be achieved with the 4 m long column which is translated to a peak capacity value approaching 10^3 on a human serum tryptic digest (Fig. 6). This illustrates that these long columns can be very useful for the analysis of complex mixtures common in proteomics and metabolomics. When considering absolute performance, one can only benefit from these long columns compared to shorter columns when operating at sufficiently large gradient times (roughly $t_g > 400$ min for the applied conditions in the present contribution). With respect to peak productivity, the shortest column even showed superior performance over the longer columns at low gradient times (roughly $t_g = 90$ min) whereas the opposite trend was observed for longer gradient times (roughly $t_g > 600$ min). Therefore, the choice of the gradient time is of high importance to get the most out of these long columns.

Furthermore, the different investigated column fragments were compared regarding flow resistance and chromatographic performance. They exhibited similar flow resistance as well as chromatographic performance that was in good agreement with gradient elution theory. From these observations it can be concluded that, presently, it is possible to produce long monolithic silica capillary columns ($L = 4$ m) displaying structural homogeneity over the entire length.

Acknowledgements

H.E. gratefully acknowledges a research grant from the Research Foundation—Flanders (FWO Vlaanderen).

The monolithic capillary column, fabricated at Kyoto Monotech, Kyoto, Japan, was kindly donated by GL Sciences Inc. as research sample.

References

[1] K. Nakanishi, N. Soga, J. Am. Ceram. Soc. 74 (1991) 2518.
[2] K. Cabrera, J. Sep. Sci. 27 (2004) 843.
[3] G. Guiochon, J. Chromatogr. A 1168 (2007) 101.
[4] H. Saito, K. Kanamori, K. Nakanishi, K. Hirao, Y. Nishikawa, H. Jinnai, Colloid Surf. A 300 (2007) 245.
[5] T. Hara, H. Kobayashi, T. Ikegami, K. Nakanishi, N. Tanaka, Anal. Chem. 78 (2006) 7632.
[6] K. Miyamoto, T. Hara, H. Kobayashi, H. Morisaka, D. Tokuda, K. Horie, K. Koduki, S. Makino, O. Nunez, C. Yang, T. Kawabe, T. Ikegami, H. Takubo, Y. Ishihama, N. Tanaka, Anal. Chem. 80 (2008) 8741.
[7] K. Sandra, M. Moshir, F. D'hondt, K. Verleysen, K. Kas, P. Sandra, J. Chromatogr. B 866 (2008) 48.
[8] K. Sandra, M. Moshir, F. D'hondt, R. Tuytten, K. Verleysen, K. Kas, I. François, P. Sandra, J. Chromatogr. B 877 (2009) 1019.
[9] B. Barroso, D. Lubda, R. Bischoff, J. Proteome Res. 2 (2003) 633.
[10] L. Xiong, R. Zhang, F.E. Regnier, J. Chromatogr. A 1030 (2004) 187.
[11] Q. Luo, Y. Shen, K.K. Hixson, R. Zhao, F. Yang, R.J. Moore, H.M. Mottaz, R.D. Smith, Anal. Chem. 77 (2005) 5028.
[12] M. Iwasaki, S. Miwa, T. Ikegami, M. Tomita, N. Tanaka, Y. Ishihama, Anal. Chem. 82 (2010) 2616.
[13] M.H. van de Meent, G.J. de Jong, J. Sep. Sci. 32 (2009) 487.
[14] K. Sandra, K. Verleysen, C. Labeur, L. Vanneste, F. D'hondt, G. Thomas, K. Kas, K. Gevaert, J. Vandekerckhove, P. Sandra, J. Sep. Sci. 30 (2007) 658.
[15] J.W. Dolan, L.R. Snyder, N.M. Djordjevic, D.W. Hill, T.J. Waeghe, J. Chromatogr. A 857 (1999) 1.
[16] X. Wang, D.R. Stoll, P.W. Carr, P.J. Schoenmakers, J. Chromatogr. A 1125 (2006) 177.
[17] N. Marchetti, G. Guiochon, Anal. Chem. 77 (2005) 3425.
[18] U.D. Neue, J. Chromatogr. A 1079 (2005) 153.
[19] Y. Shen, R. Zhang, R.J. Moore, J. Kim, T.O. Metz, K.K. Hixson, R. Zhao, E.A. Livesay, H.R. Udseth, R.D. Smith, Anal. Chem. 77 (2005) 3090.
[20] P. Sandra, G. Vanhoenacker, J. Sep. Sci. 30 (2007) 241.
[21] X. Wang, W.E. Barber, P.W. Carr, J. Chromatogr. A 1107 (2006) 139.
[22] M.H. van de Meent, G.J. de Jong, Anal. Bioanal. Chem. 388 (2007) 195.
[23] X. Wang, D.R. Stoll, A.P. Schellinger, P. Carr, Anal. Chem. 78 (2006) 3406.
[24] U.D. Neue, J. Chromatogr. A 1184 (2008) 107.